Adaptive Facet Selection in Multidimensional Hosting Capacity Region Assessment

Sicheng Gong and J. F. G. Cobben
Department of Electrical Engineering, TU Eindhoven, Netherlands
{s.gong, j.f.g.cobben}@tue.nl

***Abstract*—The hosting capacity region defines a joint feasible region in the operational space involving various installations. By facilitating their coordinated operation, this region succeeds in tapping into the grid's power delivery potential. Meanwhile, when approximating this region using an expansive polytope, facet selection should be carefully considered. Random facet selection will cause the Matthew effect, indicating that a facet which was more frequently selected owns a higher likelihood of being selected again. Such effect eventually harms the region expansion efficiency. Beyond static facet selection measures, this paper proposes adaptive measures for further improved assessment performances. The adaptive scheme is engineered to cyclically use original measures, thereby merging and leveraging their potentials on efficient facet selection. Relevant 3-dimensional region assessment experiments are conducted on a 10.5 kV Dutch grid case, which is modelled on Pandapower toolkit. The results demonstrate that, compared to static alternative measures, adaptive measures contribute to larger region space consistently, with potential region space gain being up to 62.2%. This validates the superior efficacy of adaptive mechanism in facet selection for region assessment.**

***Index Terms*—hosting capacity, feasible region, computational geometry, metaheuristic, reinforcement learning.**

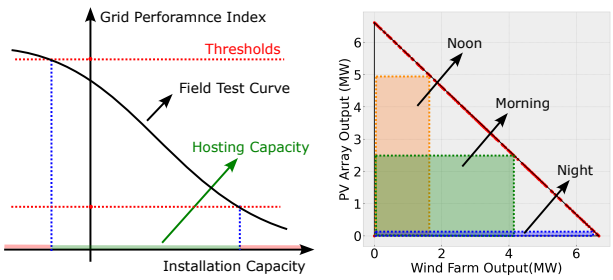

(a) Hosting capacity concept (b) Hosting capacity region

Fig. 1: The conceptual evolution of hosting capacity

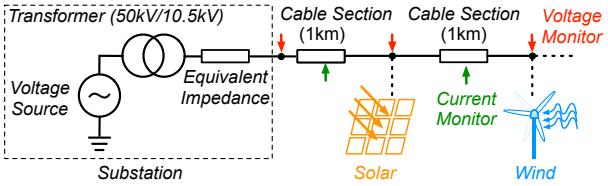

Fig. 2: 3-Node testing case schematic

I. Introduction

The concept of hosting capacity has been widespread utilized to establish integration capacity limits for various distribution energy resources [1]. With raising appliance diversity in contemporary distribution grids, hosting capacity can be extensively applied to bidirectional units such as transformers and EV charging stations [2],[3]. During hosting capacity assessment, as illustrated in Fig. 1a, the distribution system operator (DSO) adopts a risk-averse approach, focusing on extreme scenarios to define a safe operation range. This approach helps maintain constrained grid performance indices, thereby meeting power quality requirements and preventing grid overload [4], though it has compromised grid elasticity. There is a need for the hosting capacity to be intelligently restructured to maximize grid utility. In the Netherlands, the DSO is anticipating smart capacity allocation, especially given that new customers in Dutch provinces are facing extensive connection delays until years-long grid expansion [5]-[7].

Submitted to the 23rd Power Systems Computation Conference (PSCC 2024). This work was supported by NEON (New Energy and mobility Outlook for the Netherlands, with project number 17628), a cross-over project financed by NWO (the Dutch Research Council).

To this end, with the aim of leveraging grid power delivery potential, the DSO has experimentally implemented dynamic hosting capacity allocation [8]-[10]. As demonstrated by an exemplary grid case in Fig. 2, after daylight hours, the DSO reduces the hosting capacity allocated for solar plants, thereby temporarily allowing higher power injection from wind plants during the night. Such practice equivalently results in dynamic rectangular operation areas as depicted in Fig. 1b, where each interior point corresponds to a combinational operation scenario of various units. These areas are constrained by red marginal operation points, whose corresponding grid performance indices are on the edge. These boundary points formulate a quasi-triangle area named "hosting capacity region" (HCR), encompassing all potential outcomes of hosting capacity allocation [11]. Evolving from the hosting capacity concept, through coordinated cooperation across associated energy units, the HCR allows certain point of connections (POCs) to intermittently transmit more power when the remaining ones are not heavily burdened. By adopting this strategy of HCR-based collaborative cooperation, the grid power delivery potential will be fully unleashed.

Suffering convexity absence in the power grid model, the derivation of HCR can be difficult [12]. Meanwhile, as inves-

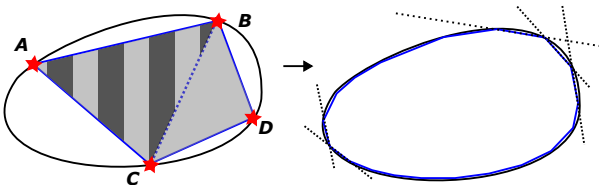

Fig. 3: Asymptotic representation of Convex region

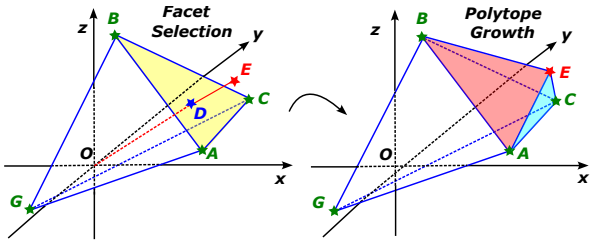

Fig. 4: Growth principle of polytope-approximated region

tigated in [13], an alternative convex region with acceptable inaccuracies can be used to approximate the HCR. This convex region can be asymptotically represented by an expansive convex hull of derived marginal points [14]. As shown in Fig. 3, to approximate the exemplary oval region, we can initially figure out three marginal points A, B, C to outline a stripe triangle as a feasible region, which later evolves into a grey quadrangle upon adding a new vertex D. By that analogy, a well-grown polytope emerges to represent the original HCR with tolerable region space loss. The polytope described by linear constraints is convenient for computer processing.

A three-dimensional (3D) case in Fig. 4 further explains the polytope growth process during HCR assessment. Regarding a known feasible region with vertices G, A, B, C, through choosing the centroid D of face $\overline{ABC}$, vector $\overline{OD}$ will be stretched to reach a new marginal point E. Afterwards, yellow plane $\overline{ABC}$ will be replaced by new planes $\overline{ABE}$, $\overline{ACE}$, and $\overline{BCE}$. Intuitively, the selected facet centroid D determines the polytope growing direction, thus influencing its growth performance. Therefore, selecting the right facets is crucial. Without proper facet selection measure, random facet selection will cause Matthew effect, where facets that have acquired enough exploitation chances is reversely easier to be selected for further exploitation. Plainly, the rich get richer and the poor get poorer. This issue and its implications for expansion efficiency will be further discussed and analyzed at Section II-C in this paper [15]. Therefore, in this illustratory case, we need certain measures to rationalize the choice of exploiting $\overline{ABC}$, rather than three other facets.

In pursuit of efficient facet selection, several static measures have been proposed in [13]. There are two aspects to evaluate the measure quality, including measure computation hardness and respective polytope hypervolume increment. None of the measures above can excel in both aspects. This paper aims to address such challenge by adaptive measure selection, drawing inspiration from adaptive ideologies in both large neighborhood search algorithm for vehicle routing problem and reinforcement learning for K-armed bandit problem [16],[17]. Through cyclically adopting static measures in reference to online updating weight factors, adaptive facet selection measures are derived to achieve a trade-off between region assessment performance and computation burden. The main contributions of this paper are twofold:

1) To answer the importance of facet selection measure adoption, we offer a theoretical analysis on the Matthew effect under random facet selection, a topic not thoroughly explored in current literature.
2) Inspired by metaheuristic and reinforcement learning techniques, we improve the facet selection efficiency via adaptive measure usage. This leads to faster polytope expansion with consistently low computational load.

The remainder of this paper are organized as follows. Section II introduces the assessment framework and provides deep discussions on Matthew effect caused by random facet selection. Based on original static facet selection measures, the adaptive variants are proposed and analyzed in Section III. Measure validation by experimental tests are conducted in Section IV and a conclusion is provided in Section V.

II. Hosting Capacity Region and Its Assessment

A. Convex region assessment

The multidimensional hosting capacity region assessment scheme in distribution grids has been briefly investigated in [13]. Respective testing cases reveal the acceptable accuracy of convexified DistFlow model as illustrated in (1), which is adopted as the grid model in this paper. Relevant variable and parameter notations are listed in Table I.

$$P_{ij} = \sum_{k:(j,k)\in E} P_{jk} - P_j \tag{1a}$$

$$Q_{ij} = \sum_{k:(j,k)\in E} Q_{jk} - Q_j \tag{1b}$$

$$v_j = v_i - 2(r_{ij}P_{ij} + x_{ij}Q_{ij}) \tag{1c}$$

$$P_{ij}^2 + Q_{ij}^2 \le v_i l_{ij}^{max} \tag{1d}$$

$$v_j^{min} \le v_j \le v_j^{max} \tag{1e}$$

$$P_i^{min} \le P_i \le P_i^{max} \ , \ Q_i^{min} \le Q_i \le Q_i^{max} \tag{1f}$$

Index	Meaning
	Constant Parameters
E / (j,k)	*Grid graph / Connection between node j and node k*
r_{ij} / x_{ij}	*Line resistance / reactance between node i and node j*
P_i^{min} / P_i^{max}	*Minimum / Maximum of active power in node i*
Q_i^{min} / Q_i^{max}	*Minimum / Maximum of reactive power in node i*
v_i^{min} / v_i^{max}	*Minimum / Maximum of voltage level square on node i*
l_{ij}^{max}	*Maximum of current magnitude square from i to j*
	Decision Variables
P_i	*Equivalent injection active power in node i*
Q_i	*Equivalent injection reactive power in node i*
v_i	*Square of voltage level over node i*

TABLE I: General notations in DistFlow model

From a risk-averse perspective, we can also employ iterative intersections between several convex polytopes produced by

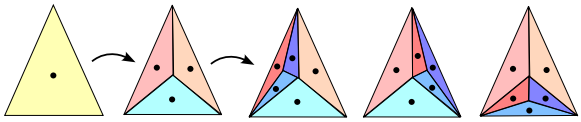

Fig. 5: Increasing descendants during facet exploitation

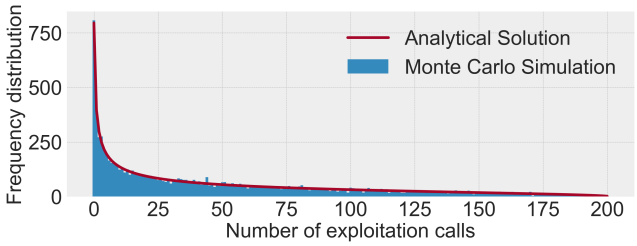

Fig. 6: Exploitation call number distribution of an initial facet

various convex models including (1), thereby ensuring an inner approximated HCR [13], within which all operation points should theoretically maintain grid feasibility. However, regardless of the chosen approach, it is inevitable to assess the convex feasible region of (1). In the remainder of this paper, we will focus on how to efficiently assess the region based on (1) through an approaching polytope.

B. Random polytope approximation for convex body

In the context of convex HCR, its assessment task converts into a general convex body approximation problem. However, identifying a finite set of marginal points while minimizing convex body approximation loss poses a significant challenge. Reference [18] provides an overview on state-of-the-art results on convex body approximation by random polytope, highlighting key findings on the limits of approximation accuracy. Specifically, an improved random walk algorithm was proposed in [19], which limits relative error after finding $O(D^7)$ points, where D is the dimension number. Such high computation burden harms its universal applicability.

In practice, the DSO prefers a heuristic approximation scheme to manage computational demands, even if it means compromising on accuracy. As detailed at Section I, a method involving endogenous polytope expansion is favored over random point search. During this expansion phase, selecting facets is a crucial step that must be approached with care, considering its potential impacts on region assessment performance.

C. Matthew effect under random facet selection

Inheriting the randomness ideology in previous approximation algorithms, a spontaneous random facet selection scheme can be considered. However,this approach may suffer Matthew effect. The concept of "Matthew effect" was initially proposed by [15] in the sociology field, delivering the idea that a greater level of initial wealth allows individuals to secure a first-mover advantage. This effect can be summarized by the platitude "the rich get richer and the poor get poorer". In the facet selection problem, the Matthew effect indicates that certain facets gain an increasing priority of being selected due to the cumulative advantage in their descendant number.

For further illustrations, we revisit face $\overline{ABC}$ in Fig. 4, depicted as a yellow plane in Fig. 5. In the initial round, face $\overline{ABC}$ has a $\frac{1}{4}$ chance of being picked, and later being replaced by three descendants in Fig. 5. These new faces, along with the original ones, then have an equal opportunity to be chosen next. Consequently, the likelihood of picking a descendant of $\overline{ABC}$ becomes $\frac{1}{2}$. If one of these descendants is selected in the second round, the descendant number of face $\overline{ABC}$ will rise to five accordingly. By the third turn, the probability to select a descendant of face $\overline{ABC}$ will be up to $\frac{3}{8}$. Inductively, under random selection, once that one initial face has been exploited first, it earns higher chance to be further exploited and reaches more descendants in an accumulative way. Plainly, the rich get richer and the poor get poorer. This tendency eventually triggers the Matthew effect.

Although the Matthew effect under random facet selection has been empirically verified by Monte Carlo simulations for 3D scenarios in [13], there is still no analytical solution for its presence in multidimensional cases. To address this, we need to first derive the theoretical frequency distribution for exploiting a single initial facet. Let D and N denote the dimension and total exploitation call number, with K being the number of exploitation calls over a single initial facet. In the ith round, the selection pool includes $(D-1)i+2$ facets, so the total possibility number S_N can be calculated as (2a). Towards a certain initial facet, if it has been exploited K times after N iterations, its descendant number will grow into $(D-1)(K-1)+1$. Therefore, the total possibility number S_K for these favorable K iterations can be derived as (2b). In remaining $N-K$ rounds, the total possibility number S_M to exploit left D initial facets is calculated as (2c). Therefore, the probability P_K for K calls occurring for a certain initial facet can be calculated as (2d).

$$S_N = \prod_{i=1}^{N} \left[(D-1)i+2\right] \tag{2a}$$

$$S_K = \begin{cases} \binom{K}{N} \prod_{i=1}^{K} \left[(D-1)(i-1)+1\right] & K>0 \\ 1 & K=0 \end{cases} \tag{2b}$$

$$S_M = \begin{cases} \prod_{i=1}^{N-K} \left[(D-1)i+1\right] & N>K \\ 1 & N=K \end{cases} \tag{2c}$$

$$P_K = \frac{S_K \cdot S_M}{S_N} \tag{2d}$$

To verify such analytical solution, we conducted 10000 simulations with setting D and N as 3 and 200. The distribution of K has been plotted by blue bars in Fig. 6. Simultaneously, the estimated distribution based on (2d) is given by red curve in the same figure, showing a good fit with the empirical data. The validity of (2) has been successfully confirmed. Based on these analytical results, the probability $\Gamma_{12.5\%}$ that an initial face acquires less than 12.5% exploitation chances, a half of what would be expected if chances were evenly distributed among all four initial facets, can be calculated as high as

44.58%. Conversely, the probability $(1-\Gamma_{50\%})$ that it acquires more than 50% exploitation chances, which doubles the corresponding expected value, is up to 18.09%. Through tuning the values of D and N in (2), similar phenomena of high $\Gamma_{\frac{1}{2(D+1)}}$ and $(1-\Gamma_{\frac{2}{D+1}})$ values keep being observed, thereby analytically confirming the existence of Matthew effect under random facet selection.

The Matthew effect under random facet selection leads to irrational distribution of exploitation calls, where certain initial facets might not be chosen in enough times, adversely influencing the HCR assessment performance. As investigated in [13], blaming on Matthew effect, sharing the same value of N, random facet selection will cause at most 21.13% region space loss compared to measure-based ones. The results highlight the necessity of measure-based facet selection, whose respective selection measures will be further discussed and explored at Section III.

III. Adaptive facet selection

A. Static selection measures

In need of measure-based facet selection, several static measures have been proposed in [13]. Those static measures are designed to eliminate the hidden issue of Matthew effect, they lead to lower measure values for the descendants of initially well-exploited facets as the polytope expands.

1) Local-greedy measure: As listed in Table II, let $\Delta\mathcal{R}$ denote the additional region hypervolume after facet selection and exploitation. By adopting a local-greedy approach, which seeks the highest immediate benefit in each step, we can take $\Delta\mathcal{R}$ as the criterion for selecting facets in a straightforward way. Meanwhile, due to its ergodic nature, this greedy measure may be questioned in the aspect of computation hardness, which needs to exploit all D new facets in every iteration. Each turn of facet exploitation, particularly using the bisection method, is time-consuming due to inevitable iterative power flow analysis. In a general multidimensional HCR assessment task, such computational demands become untenable, despite the leading performance of this measure as investigated in [13]. Therefore, the local-greedy measure needs alternatives to cope with limited computing resource in most practices.

Measure	Meaning in 3D case	Target
$\Delta\mathcal{R}$	Polyhedron volume increment	Maximal
$\mathcal{V}(\mathcal{F})$	Face area	Maximal
$\mathcal{V}(\mathcal{C}(\mathcal{F},\mathcal{O}))$	Origin-apex triangular pyramid volume	Maximal
$\boldsymbol{g}(\mathcal{F})$	Face generation order	Minimal

TABLE II: Measure table for facet selection

2) Alternative measure: For measure computation burden reduction, as proposed in [13], several alternative measures can be considered as listed in Table II. Regarding n-dimension polytope $\mathcal{C}$, let $\mathcal{F}$ denote its facet, which is an $(D-1)$-dimension polytope. $\mathcal{C}(\cdot)$ computes a convex-hull of all inputs. $\mathcal{V}(\cdot)$ calculates the polytope hypervolume. $\boldsymbol{g}(\cdot)$ enumerates the facet generation order, and equals 0 for initial $(D+1)$ facets. In the 3D context, a higher $\mathcal{V}(\mathcal{F})$ indicates a larger basis of the new generated pyramid, and a higher $\mathcal{V}(\mathcal{C}(\mathcal{F},\mathcal{O}))$ implies a pyramid basis far from the origin point. Both results empirically contribute to faster polytope growth. $\boldsymbol{g}(\mathcal{F})$ aims for brute-force Matthew effect mitigation without any geometric considerations. Notably, in some extreme cases, the facet selected by $\mathcal{V}(\mathcal{F})$ or $\mathcal{V}(\mathcal{C}(\mathcal{F},\mathcal{O}))$ may be stuck in an looping situation, where one newly generated descendant facet is quite close and similar to its ancestor facet. This occurs particularly when the ancestor facet, which possesses a large hypervolume, is positioned too near to the origin. To jump off this predicament, one approach could be to exclude this descendant facet from the selection pool directly.

The alternative measures outlined above eliminate the need for preliminary facet exploration, thus substantially lowering computational complexity. Meanwhile, compared to $\Delta\mathcal{R}$, they are more empirical and own weaker causal relationship with efficient facet selection, which in turn can impact HCR assessment performances. Moreover, since these measures are static, they lack adaptive properties to maintain consistent performances across various scenarios. Therefore, it is crucial to consider an adaptive framework to catalyze the reaction between those static measures.

B. Primal adaptive measure design

Although static alternative measures at Table II maintain consistent computation hardness, they may contribute to inconsistent facet selection efficiency during region assessment. In other words, in a general case, neither of them can consistently outperforms the others in terms of providing a theoretically guaranteed enhanced assessment. Intuitively, these measures are expected to be combined in a certain way for merging and leveraging their potentials on efficient face selection. Therefore, inspired by adaptive ideology in large neighborhood search algorithm for vehicle routing problems, adaptive measure selection can be adopted [16],[20]. Beside the contribution to potential faster region expansion, this adaptive mechanism owns another advantage of previous knowledge omittance on the candidate case. This allows the DSO to eliminate worries about choosing the appropriate static measure for the upcoming test case.

Let $\omega_m^{(i)}$ be the weight factor of measure m used in i-th iteration in (3). α is a adaptive coefficient in range [0,1]. $\Omega_m^{(i)}$ is the score of measure m in that round, which can be defined as polytope hypervolume gain once choosing measure m. The measure with the maximal weight factor will be choose for helping facet selection. This adaptive scheme aims to continuously evaluate and learn from historic and present performances of each static measure, thereby picking out a suitable measure to fit the current assessment process.

$$\omega_m^{(i)} \leftarrow (1-\alpha)\omega_m^{(i-1)} + \alpha\Omega_m^{(i)} \tag{3}$$

In summary, Algorithm 1 is proposed for primal adaptive facet selection in region assessment. The naming of "primal" for Algorithm 1, is based on its concise deterministic measure

selection mechanism without either perturbative or probabilistic ideology, which is more popular in complex adaptive mechanism and will be discussed at Section III-C.

Algorithm 1: Primal adaptive measure selection

Data: Measure list **M**, polytope feasible region $\mathcal{C}$.
Set $\omega_m^{(0)} \leftarrow 0$ for m in **M**;
Initialize an adaptive coefficient α;
Initialize iteration number $i \leftarrow 1$;
repeat
  for m *in* ***M*** **do**
    Set $\mathcal{C}_m$ to be a polytope from $\mathcal{C}$, which uses m as the facet selection measure;
    $\Omega_m^{(i)} \leftarrow \mathcal{V}(\mathcal{C}_m) - \mathcal{V}(\mathcal{C})$;
    $\omega_m^{(i)} \leftarrow (1-\alpha)\omega_m^{(i-1)} + \alpha\Omega_m^{(i)}$;
  end
  $\mathcal{C} \leftarrow \mathcal{C}_m$, where respective $\omega_m^{(i)}$ is maximal;
  (finalizing facet selection in each round)
until *stopping criterion reaches*;

Based on measure list **M**, this adaptive measure exhibits higher computation hardness than a single static measure. It exploits all facets in the waiting pool preliminarily, which are nominated by individual measures in **M** during each cycle. However, only one measure is ultimately selected for use based on weight factors. Noticeably, the pool size will not increase by $|\mathbf{M}|$ iteratively, because measures may recommend the facet already in the waiting pool. Therefore, regardless of the dimension number D, its exploitation call number threshold in each iteration is capped at $|\mathbf{M}|$. Compared to static local-greedy measure, in a general multidimensional case, the computation hardness can be substantially reduced through primal adaptive measure.

C. Reinforcement-learning-inspired adaptive measures

Enlightened by reinforcement learning methods in K-armed bandit problem, the primal adaptive measure evolves upon integrating concepts of perturbation or probability [21]. The K-armed bandit problem, a fundamental issue in reinforcement learning, seeks for an optimal strategy to allocate limited resources between various choices with the maximal expected reward [17]. As an analogy, looking into the facet selection problem during region assessment, we need to invest limited facet exploitation chances based on various facet selection measures, aiming to maximize the final region space.

Based on model similarity between these two problems, their respective algorithmic solutions should have common elements. Noticeably, the primal adaptive selection strategy described in Section III-B can be taken as a variant of incremental action-value method, which has been widespread adopted to cope with the K-armed bandit problem. In such context, the introduction of perturbative or probabilistic ideology holds promise for enhancing the region assessment performance, drawing from their proven effectiveness in the K-armed bandit problem.

1) ϵ-greedy adaptive measure: Rooted in the perturbative ideology, inheriting and devising the deterministic mechanism from the primal adaptive measure, ϵ-greedy mechanism allows intermittent random choice with the probability of ϵ. Accordingly, Algorithm 1 evolves into Algorithm 2 for ϵ-greedy adaptive measure implementation. The ϵ-greedy adaptive measure aims for a trade-off between "exploitation" of the measure owning the highest expected payoff and "exploration" to acquire more information about the expected payoffs of the other measures. Unlike direct random facet selection with the hidden issue of Matthew effect, the randomness of selection acts on the static measures. Under ϵ-greedy adaptive mechanism, the waiting pool for selection can still incorporate up to $|\mathbf{M}|$ new facets in each iteration, avoiding the excessive inclusion characteristic of entirely random selection.

Algorithm 2: ϵ-greedy adaptive measure selection

Data: Input data in Algorithm 1, probability ϵ.
Implement initialization steps in Algorithm 1;
repeat
  Run the repeat-loop section in Algorithm 1;
  Generate a random number τ in range [0,1];
  if $\tau \leq \epsilon$ **then**
    $\mathcal{C} \leftarrow \mathcal{C}_n$, where n is a random integer in **M**;
  end
until *stopping criterion reaches*;

The computation hardness of ϵ-greedy adaptive measure keeps the same with that of primal one. However, the intermittent random nature of ϵ-greedy adaptive measure introduces more uncertainties to region assessment performance, as ϵ also needs to be tuned besides α. Such additional strain of tuning the perturbation degree is undesirable. Therefore, instead of perturbative ideology, probabilistic ideology can be integrated, whose probabilistic distribution can be determined in advance to omit extra parameter tuning.

2) Gradient adaptive measure: Instead of weight-factor-dominating framework in primal and ϵ-greedy ones, a probabilistic preference framework is adopted in gradient adaptive measure. Instead of absolute priority, a larger weight factor implies a higher likelihood to select the respective measure. For the ith iteration, towards the weight factor $\omega_m^{(i)}$ for measure m, the corresponding probability $\pi_m^{(i)}$ can be calculated as (4) using the soft-max distribution, a classic function utilized in K-armed bandit problem [17]. It should be noted that the probability function can be also flexible, including sparsemax, spherical softmax, etc [22]. However, to maintain focus and avoid complexity, this paper only explores and validates the use of the softmax function for region assessment.

$$\pi_m^{(i)} = \frac{e^{\omega_m^{(i)}}}{\sum_{m=1}^{|\mathbf{M}|}\left(e^{\omega_m^{(i)}}\right)} \tag{4}$$

Based on variable notations in primal adaptive measure part, upon calculating the average reward $\overline{\Omega_i}$ in previous i iterations as (5) , the weight factor update rule is written as

(6). $\overline{\Omega_i}$ serves as a baseline to determine whether the selected measure m should earn more preference in the next round. In accordance with (4)-(6), Algorithm 3 is derived for gradient adaptive measure implementation.

$$\overline{\Omega_i} = \frac{\sum_{j=1}^{i} \Omega_j}{i} \tag{5}$$

$$\begin{aligned} \omega_m^{(i)} &\leftarrow \omega_m^{(i-1)} + \alpha(\Omega_i - \overline{\Omega_i})(1 - \pi_m^{(i)}), \quad m = A_i \\ \omega_m^{(i)} &\leftarrow \omega_m^{(i-1)} - \alpha(\Omega_i - \overline{\Omega_i})\pi_m^{(i)}, \quad m \neq A_i \end{aligned} \tag{6}$$

Algorithm 3: Gradient adaptive measure selection

Data: Input data in Algorithm 1.
Implement initialization steps in Algorithm 1;
repeat
  for m *in* $\boldsymbol{M}$ **do**
    $\pi_m^{(i)} \leftarrow \frac{e^{\omega_m^{(i)}}}{\sum_{m=1}^{|\mathbf{M}|}\left(e^{\omega_m^{(i)}}\right)}$;
  end
  Select n in $\mathbf{M}$ using π values (Gibbs-distribution);
  Set $\mathcal{C}_n$ to be a polytope from $\mathcal{C}$, which uses n as the facet selection measure. $\mathcal{C} \leftarrow \mathcal{C}_n$;
  $\Omega_i \leftarrow \mathcal{V}(\mathcal{C}_n) - \mathcal{V}(\mathcal{C})$, $\overline{\Omega_i} \leftarrow \frac{\sum_{j=1}^{i} \Omega_j}{i}$;
  for m *in* $\boldsymbol{M}$ **do**
    if *m=n* **then**
      $\omega_m^{(i)} \leftarrow \omega_m^{(i-1)} + \alpha(\Omega_i - \overline{\Omega_i})(1 - \pi_m^{(i)})$;
    else
      $\omega_m^{(i)} \leftarrow \omega_m^{(i-1)} - \alpha(\Omega_i - \overline{\Omega_i})\pi_m^{(i)}$;
    end
  end
until *stopping criterion reaches*;

Without pre-exploitation in the waiting pool of facets, which aims for their expected pay-off evaluation, the gradient adaptive measure is designed to learn after the action. Therefore, the respective facet exploitation call number in each iteration has been further reduced to 1, which equals that of static measures. In other words, its computation hardness keeps the same with those of static alternative measures, which is lower than those of primal and ϵ-greedy ones.

D. Summary

To encapsulate thee characteristics of all facet selection measures reviewed, Table III provides a comparative overview, where n_e denotes the facet exploitation call number in each iteration. The "Performance" column highlights their contributions to region assessment performance. The property values in this column indicate their empirical performance, which is subject to further exploration and validation at Section IV.

IV. Experimental Validation

Numerical tests are implemented to verify the effectiveness of proposed adaptive measures. The grid case in Fig. 7 is based on a 10.5 kV network model from a Dutch DSO, Alliander [23]. All POCs connects with constant-power loads,

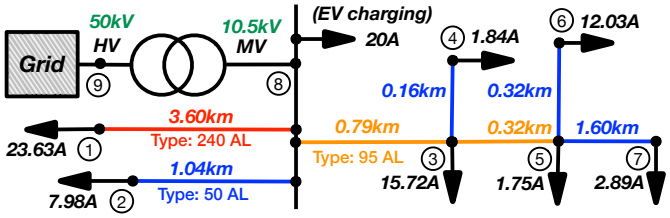

Fig. 7: The schematic of testing grid case

Measure	Adaptive	Matthew Effect	n_e	Performance
- (random)	No	Yes	1	Low
$\Delta\mathcal{R}$	No	No	D	High
$\mathcal{V}(\mathcal{F})$	No	No	1	Medium
$\mathcal{V}(\mathcal{C}(\mathcal{F}, \mathcal{O}))$	No	No	1	Medium
$g(\mathcal{F})$	No	No	1	Medium
Primal	Yes	No	$\leq \lvert\mathbf{M}\rvert$	High
ϵ-greedy	Yes	No	$\leq \lvert\mathbf{M}\rvert$	High
Gradient	Yes	No	1	High

TABLE III: Comparisons of various facet selection schemes

whose nominal current values are given in Fig. 7 with the power factor being 0.98. More grid parameters are provided in Table IV. Bus 2,4,7 or 3,5,7 are considered for three additional EV charging station integration. To maximize converter utility, we select injected active power from these three POCs as dimensions.The fundamental vectors to formulate an initial region are [1,0,0], [0,1,0], [0,0,1] and [-1,-1,-1]. The measure list M used in each adaptive measure includes all three static alternative measures. Both learning ratio α and perturbation degree ϵ are set to be 0.1 as recommended in [17].

Object (max current)	Resistance	Reactance (50Hz)
240 AL Cable (412A)	126 mΩ/km	116 mΩ/km
150 AL Cable (312A)	320 mΩ/km	188 mΩkm
95 AL Cable (224A)	641 mΩ/km	204 mΩ/km
36MVA 50kV/10.5kV Transformer	0.0022 p.u.	0.065 p.u.

TABLE IV: Power cable and transformer parameters

A. Primal adaptive measure selection scheme

In each iteration, a facet will be selected for exploitation, and a new vertex will be generated and included in the updated region polytope. In the case of selecting POC 2,4,7 for 3D region assessment studies, as shown in Fig. 8a, in the whole progress of 400 iterations, the primal adaptive measure keeps better region assessment performance than three static alternative measures. As plotted in Fig. 8b, similar phenomena are observed in the case of POC 3,5,7 with the iteration number being 600, where the superiority of primal adaptive measure is even more pronounced.

Compared to measure $\mathcal{V}(\mathcal{F})$, which performs the best among static alternative measures, the primal adaptive measure earns 2.87% and 15.2% extra region space in these two distinct scenarios. Such divergence might be empirically understood by examining the geometric shapes of HCRs as illustrated in Fig. 9. The HCR involving POC 2,4,7 resembles an orthotope more closely. In an orthotope, only the 2^D critical

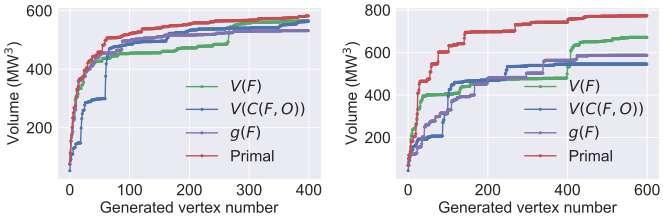

(a) $POC\ 2,4,7$ (b) $POC\ 3,5,7$

Fig. 8: Polytope growth under various measures

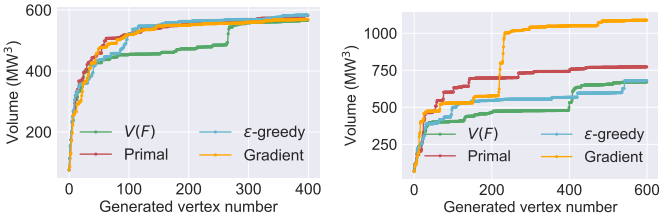

(a) $POC\ 2,4,7$ (b) $POC\ 3,5,7$

Fig. 10: Polytope growth with adaptive measures

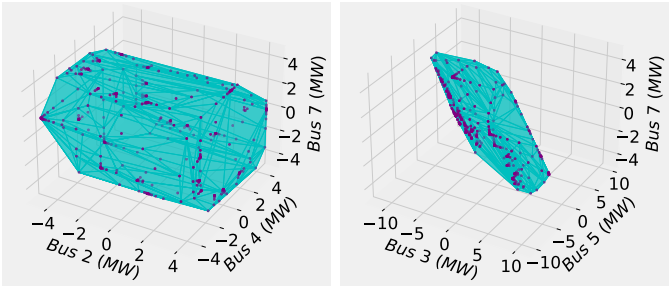

(a) $POC\ 2,4,7$ (b) $POC\ 3,5,7$

Fig. 9: Assessed hosting capacity regions

vertices exist, and the inclusion of any such vertex into the polytope can significantly contribute a significant hypervolume improvement. Intuitively, the region of POC 3,5,7 is farther from a regular shape, suggesting a stronger motivation to adopt adaptive mechanism for more frequent explorations with a broader horizon. This, in turn, increases the chance of identifying more critical vertices for better overall outcomes.

After confirming the superiority of primal adaptive measure in region assessment performance, its empirical computation complexity should be studied as well. Even though n_e owns a upper bound of 3, the total facet exploitation call numbers are only 423 and 610 in two separate cases, whose equivalent average n_e values are as low as 1.06 and 1.02. Considering such minor extra computation hardness of primal adaptive measure, its priority over static alternative ones in the whole measure pool has been further confirmed.

B. Reinforcement-learning-inspired adaptive scheme

To verify the effectiveness of ϵ-greedy and gradient adaptive measures, experiments were carried out similarly to those cases in Section IV-A. Together with previous results based on $\mathcal{V}(\mathcal{F})$ and primal adaptive measure, respective region assessment results are plotted in Fig. 10. In the case of POC 2,4,7, ϵ-greedy one leads narrowly, indicating the benefit of certain perturbation. Meanwhile, in the case of POC 3,5,7, the gradient adaptive measure leads by a huge margin. It contributes to 40.8% extra region space compared to primal one, and 62.2% extra compared to $\mathcal{V}(\mathcal{F})$. The power of probabilistic ideology in region assessment tasks has been confirmed. Simultaneously, In spite of falling behind gradient and primal ones, ϵ-greedy measure still leads narrowly with $\mathcal{V}(\mathcal{F})$ in this scenario, showcasing the general superiority of adaptive framework over static one.

In the exploitation process with gradient adaptive measure, as shown in Fig. 10b, after approximately 200 iterations, it successfully explores several critical vertices within a probabilistic framework. These critical vertices contribute significantly to such rapid region expansion. They are promising to be acquired by learning more information about the expected payoffs of various measures, emphasizing on the importance of incorporating perturbative and probabilistic mechanisms to entourage frequent "exploration".

C. Summary

In accordance with experimental results illustrated in Fig. 8 and 10, the effectiveness of all proposed adaptive measures has been successfully validated. Particularly, gradient adaptive measure stands out as the optimal option, considering its near-top performance in the case of POC 2,4,7 and substantially leading performance in that of POC 3,5,7.

V. Conclusion

Efficient facet selection is crucial for multidimensional hosting capacity region assessment. This study introduces adaptive facet selection measures that develop from traditional static approaches by employing them cyclically. Enlightened by adaptive ideology in meta-heuristics and reinforcement learning studies, the proposed measures will be able to merge and harness the strengthens of static ones. For their effectiveness validation, grid case studies have been implemented. Relevant results revealed the advantage of adaptive measures to boost region assessment performance. Compared to static alternative measures, the additional region space gain with adaptive measures can be up to 62.2%. Meanwhile, this comes with the additional strain of parameter tuning, including learning ratio α and perturbation degree ϵ.

Looking ahead, regarding these adaptive measure, comprehensive parameter sensitivity analysis will be implemented, thereby answering the impacts of these measure parameters on region assessment performance. The impact of network complexity on the computational performance will be also analyzed, using an actual larger-scale grid case involving 298 buses. Moreover, more technical paths, for instance deep reinforcement learning, will be discussed in future works, to uncover new methods for further improving intelligent facet selection strategies.

REFERENCES

[1] M. H. Bollen and F. Hassan, *Integration of Distributed Generation In The Power System*. John wiley & sons, vol. 80, 2011.

[2] S. Hajeforosh, A. Khatun and M. Bollen, *Enhancing the hosting capacity of distribution transformers for using dynamic component rating*. Int J. Electr. Power Energy Syst., 142, 108130, 2022.

[3] J. Zhu, W. J. Nacmanson, L. F. Ochoa and B. Hellyer, *Assessing the EV Hosting Capacity of Australian Urban and Rural MV-LV Networks*. Electric Power Systems Research, 212, 108399, 2022.

[4] A. Koirala, T. Van Acker, R. D'hulst, and D. Van Hertem, *Hosting capacity of photovoltaic systems in low voltage distribution systems: A benchmark of deterministic and stochastic approaches*. Renewable and Sustainable Energy Reviews, 155, p.111899, 2022.

[5] ElaadNL, *Flexpower3: Meer Laden op een Vol Elektriciteitsnet (More charging on a saturated electricity Grid)*. [Online]. Available: https://elaad.nl/wp-content/uploads/2022/11/FlexPower-Rapport.pdf.

[6] NOS Nieuws, *Weer ruimte voor grootgebruikers op stroomnet brabant en limburg (Space again for large users on the Brabant and Limburg power grid)*. [Online]. Available: https://nos.nl/artikel/2443933-weer-ruimte-voor-grootgebruikers-op-stroomnet-brabant-en-limburg

[7] A. Stawska, N. Romero, M. de Weerdt, and R. Verzijlbergh, *Demand response: For congestion management or for grid balancing?*. Energy Policy, 148, 111920, 2021.

[8] T. C. de Oliveira, *The concept of dynamic hosting capacity of distributed renewable generation considering voltage regulation and harmonic distortion*. Federal University of Itajuba, 2018.

[9] A. K. Jain, K. Horowitz, F. Ding, K. S. Sedzro, B. Palmintier, B. Mather, and H. Jain, *Dynamic hosting capacity analysis for distributed photovoltaic resources—Framework and case study*. Applied Energy, 280, 115633, 2020.

[10] M. Z. Liu, L. F. Ochoa, P. K. Wong, and J. Theunissen, J, *Using OPF-based operating envelopes to facilitate residential DER services*. IEEE Transactions on Smart Grid, 13(6), 4494-4504, 2022.

[11] S. Gong, V. Cuk, T. C. de Oliveira, and J. F. G. Cobben, *An extended hosting capacity approach including energy storage* in *Distributed Energy Storage in Urban Smart Grids*, P. F. Ribeiro and R. S. Salles, Eds., ch. 11. IET, 2022. [Online]. Available: https://research.tue.nl/en/publications/an-extended-hosting-capacity-approach-including-energy-storage

[12] M. E. Baran and F. F. Wu, *Network reconfiguration in distribution systems for loss reduction and load balancing*. IEEE Transactions on Power delivery, 4(2), pp.1401-1407, 1989.

[13] S. Gong, V. Cuk, and J. F. G. Cobben, *Multidimensional hosting capacity region in dutch MV grid congestion management*. IEEE Trans. Power Syst., 2023.

[14] G. M. Ziegler, *Lectures on polytopes (Vol. 152)*. Springer Science & Business Media, 2012.

[15] R. K. Merton, *The matthew effect in science: The reward and communication systems of science are considered*. Science, vol. 159, no. 3810, pp. 56–63, 1968.

[16] S. Ropke and D. Pisinger, *An adaptive large neighborhood search heuristic for the pickup and delivery problem with time windows*. Transportation Science, 40(4), 455-472, 2006.

[17] R. S. Sutton and G. B. Andrew, *Reinforcement learning: An introduction*. MIT press, 2018.

[18] J. Prochno, C. Schütt and E. M. Werner *Best and random approximation of a convex body by a polytope*. Journal of Complexity, 71, 101652, 2022.

[19] L. Lovász and M. Simonovits, *Random walks in a convex body and an improved volume algorithm*. Random structures & algorithms, 4(4), 359-412, 1993.

[20] D. Pisinger and S. Ropke, *Large neighborhood search* in *Handbook of Metaheuristics*, M. Gendreau and P. Jean-Yves, Eds., ch. 13. Springer, 2019.

[21] E. G. Talbi, *Machine learning into metaheuristics: A survey and taxonomy*. ACM Computing Surveys (CSUR), 54(6), 1-32, 2021.

[22] A. Laha, S. A. Chemmengath, P. Agrawal, M. Khapra, K. Sankaranarayanan, and H. G. Ramaswamy, *On controllable sparse alternatives to softmax*. Advances in Neural Information Processing Systems, 31, 2018.

[23] A. Ibós, *Defining current harmonic limits for customers connected to low and medium voltage*. M.S. thesis, Eindhoven University of Technology, Eindhoven, 2018.